China Ocean Engineering, Vol.13, No.1, pp.81 – 92.
China Ocean Press, 1999. Printed in P.R. China.

The Behaviour of LNG Carrier Moored to a Jetty Exposed to Waves, Swell, Unsteady Wind and Current

JI Chunqun* **and J. E. W. WICHERS****

Abstract — Most terminals for tankers are piers and sea islands, while other types include single point moorings and multiple-buoy moorings. The LNG and LPG carrier moored to the jetty is a very common terminal for transfer of gas in open seas. It is important to estimate the motions and line tensions of the LNG carrier when it moors to a jetty in metocean environment. Normally, the motions of the LNG carrier would be restricted by the loading arm, which is connected to LNG carrier's manifold. An example of 125,000 m^3 LNG carrier moored to a jetty exposed to a set of environment conditions is given. A mathematical model which is based on the equations of motion in the time domain is used to the analysis of LNG moored to an offshore jetty exposed to waves, swell, wind and current. By means of a time domain computer program TERMSIM computations are carried out to determine and optimize the lay-out and / or orientation of the jetty and mooring gear in terms of forces in mooring lines and fenders and the envelope of motions of the loading arms. The purpose of this study is to determine the sensitivity of the mooring system and carrier motions to the combinations of wind waves with and without swell, steady wind and wind spectra. The results can be consulted by the designer in the design of jetties.

Key words: *mooring system*; *dynamic response*; *time domain analysis*; *jetty*

1. Introduction

The worldwide increasing demand for liquid natural gas (LNG) and liquid petroleum gas (LPG) results in extensive transport from gas plants to receiving countries, thus, new jetties are being designed or built. Existing jetties are sometimes converted to receive carriers. For the design of jetties computations have to be carried out so that these carriers can be moored safely to a jetty exposed to wind waves and current. By means of the time domain computer program TERMSIM computations can be carried out to determine and optimize the lay-out and / or orientation of the jetty and mooring gear in terms of forces in mooring lines and fenders and the envelope of motions of the loading arms. In this paper a 125,000 m^3 LNG carrier is assumed to be moored to a jetty and exposed to a set of environmental conditions. The purpose of this study is to determine the sensitivity of the mooring system and carrier motions to the combinations of wind waves with and without swell, steady wind and wind spectra.

2. Calculation Model of Carrier and Jetty

The carrier will be a 125,000 m^3 LNG carrier with spherical cargo tanks. The principal dimensions of the carrier are derived from OCIMF (1985). The particulars and stability data of the carrier are given in Table 1. The general arrangement of the carrier is shown in Fig. 1. The carrier is moored to a jetty in water depth of 16 m. The lay-out of the jetty and the mooring

* Associate Professor, State Key Laboratory of Ocean Engineering, Shanghai Jiaotong University, Shanghai 200030, P. R. China
** Vice President and General Manager of MARIN USA Inc. Maritime Research Institute Netherlands, The Netherlands

system is also given in Fig. 1. The stern and stern breasting lines are connected to bollards $1^{\#}$ and $2^{\#}$. The spring lines are connected to bollards $3^{\#}$ and $4^{\#}$ and the bow brasting lines are connected to bollards $5^{\#}$ and $6^{\#}$. The lines are connected to the bollards at an elevation of 6 m above still water level. To bollards $3^{\#}$ and $4^{\#}$ fenders are attached. On each bollard two fenders are positioned 5 m apart from the centerline of the bollard at an elevation of 4 m above still water level. Each mooring line is a combi-line. A combi-line consists of a steel wire (56 mm in diameter) and a 20 m long nylon double braided tail (105 mm in diameter). In total 14 lines are employed. The positions of the fairleads and the manifold on the carrier are given in Table 2. The positions of the release hooks on the bollards and the position of the fenders are given in Fig. 1.

Table 1 Particulars and stability data

Designation	Magnitude
Length between perpendiculars L_{pp} (m)	274.0
Breath B (m)	44.2
Depth mould D (m)	25.0
Draft T (m)	11.0
Displacement volume V (m^3)	93253
Center of gravity above keel KG (m)	10.2
Metacentric height GM (m)	10.4
Longitudinal radius of gyration in air K_{YY} (m)	68.0
Transverse radius of gyration in air K_{XX} (m)	15.9
Vertical radius of gyration in air K_{ZZ} (m)	69.0
Roll period T_φ (s)	11.9
Wind area frontal A_F (m^2)	1300
Wind area side A_S (m^2)	6600

Table 2 Fairleads and manifold position (corresponding to Fig.1)

Designation	X_S^* (m)	Y_S^* (m)	Z_S^{**} (m)
Fairleads			
F_2	−140	9.5	13.0
F_3	−126	14.5	13.0
F_4	−90	21.5	13.0
F_5	100	21.5	13.0
F_6	115	17.5	13.0
F_7	130	10.0	13.0
Manifold	19.1	19.1	15

Notes: * — w. r. t. midship cross section and center; * * — w. r. t. water line.

3. Environmental Conditions in the Simulation

For this study a combination of weather conditions is applied. The purpose is to study the sensitivity of the carrier's motions to the given environmental conditions. The definitions of the

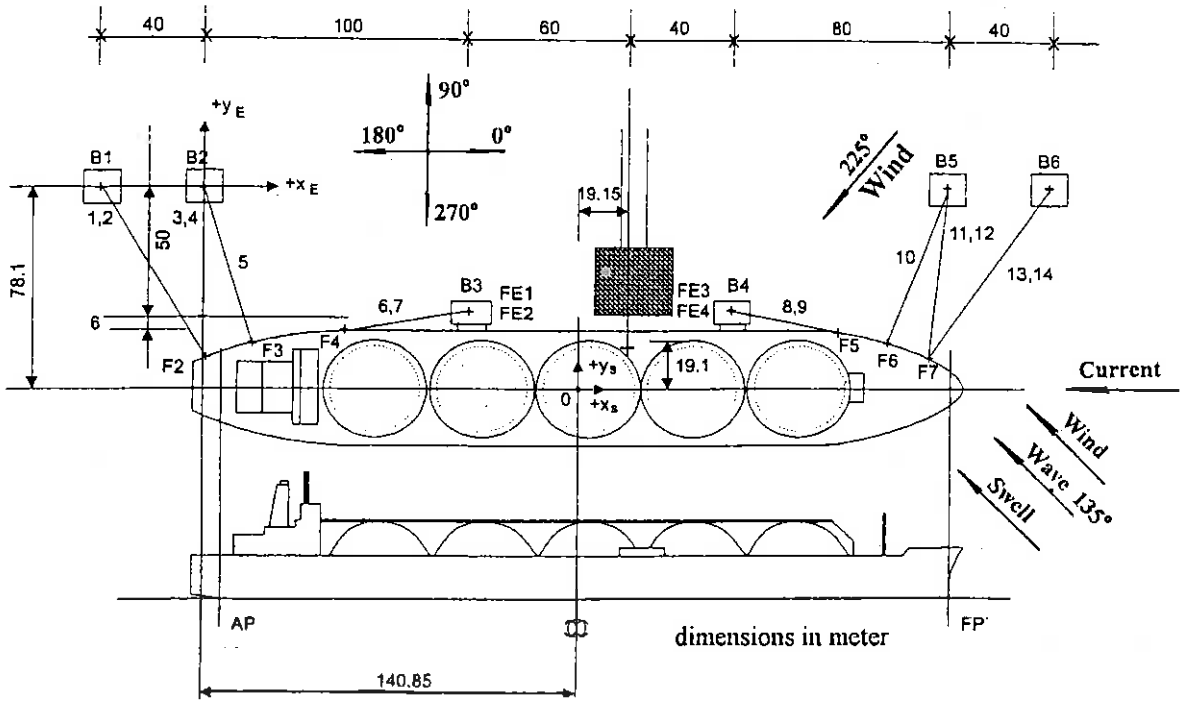

Fig. 1. Lay-out of jetty and mooring system.

wave, wind and current direction with regard to the carrier are also given in Fig. 1. As a standard case the following weather case is taken: JONSWAP wave spectrum with H_s = 2.5 m and T_1 = 9 s (135 °), a steady 15-second wind speed of 25.2 m / s (135 °) and a steady current velocity of 1.5 m / s (180 °). With respect to the standard case the following parameters are applied:

- Mean period (T_1 = 7 to 11 s) with H_s = 2.5 m;
- The API-wind spectrum with a mean hourly wind speed of 20 m / s instead of a steady 15 s wind speed;
- The JONSWAP spectrum with H_s = 2.0 m and T_1 = 9 s in association with a Gaussian swell spectrum with H_s = 0.5 m and T_1 = 17 s;
- Computations (with the mean period T_1 = 9 s) are repeated, while the wind direction is changed to 225 ° .

In simulations the API wind spectrum, JONSWAP wave spectrum and Gaussian swell spectrum are used as the input of environment condition. The corresponding formulas are given as follows. A review of the computer simulations is given in Table 3.

— API wind spectrum:

$$S_V(\omega) = \frac{\sigma_V^2}{2\pi \cdot f_p} \left[1 + \frac{1.5}{2\pi} \cdot \frac{\omega}{f_p}\right]^{-\frac{5}{3}} \tag{1}$$

in which ω — frequency in rad / s of wind oscillation; S_V — spectral density of wind speed in m^2 / s; V — hourly mean wind speed; f_p — average factor: 0.0025 V; σ_V — turbulence intensity, σ_V = 0.164 V.

— JONSWAP wave spectrum:

$$S_\zeta(\omega) = \alpha \cdot (g^2 \omega^{-5}) e^{-1.25(\frac{\omega_m}{\omega_m})^4} \gamma \cdot e^{-(\omega-\omega_m)^2/(2\sigma^2\omega_m^2)} \tag{2}$$

in which: γ — peak parameter ($\gamma = 3.3$); $\sigma = 0.07$ for $\omega \leqslant \omega_m$, and $\sigma = 0.09$ for $\omega > \omega_m$; ω_m — Modal frequency; $\alpha = 0.076\ (g \cdot d/U^2)^{-0.22}$; U = mean wind speed (knots); g — acceleration of gravity (m / s^2).

— Gaussian swell spectrum:

$$S_\zeta(\omega) = \frac{(\frac{\zeta_{w\frac{1}{3}}}{4})^2 \cdot e^{-50(\frac{\omega}{\omega_p}-1)^2}}{0.1\omega_p\sqrt{2\pi}} \tag{3}$$

in which $\zeta_{w\frac{1}{3}}$ — significant wave height in m; $\omega_p = 2\pi / T_p$; T_p — peak period in s.

Table 3 Review of computations

Run case	Wave			Swell			Wind			Current
	α_{WA} (°)	H_s (m)	T_1 (s)	α_S (°)	H_s (m)	T_1 (s)	α_{WI} (°)	V_W (m / s)	V_{WAPI} (m / s)	V_C (m / s)
1	135	2.5	11				135	25.2		1.5
2	135	2.5	9				135	25.2		1.5
3	135	2.5	7				135	25.2		1.5
4	135	2.5	9				135		20.0	1.5
5	135	2.0	9	135	0.5	17	135	25.2		1.5
6	135	2.0	9	135	0.5	17	135		20.0	1.5
7	135	2.5	9				225	25.2		1.5
8	135	2.5	9				225		20.0	1.5
9	135	2.0	9	135	0.5	17	225	25.2		1.5
10	135	2.0	9	135	0.5	17	225		20.0	1.5

The wind speed as a function of height above the mean water level and average time interval is approximated by the following power law:

$$V_W(t, z) = \alpha V_W (\frac{z}{10})^\beta \tag{4}$$

in which $V_W(t, z)$ — wind speed averaged over a time interval t as defined by α and β, z meter above the mean water level; V_W — wind speed averaged over one hour, 10 m above sea level; α — guest factor referenced to V_W; β — height exponent.

The factors in the power law for the wind profiles are shown in Table 4.

Table 4 Factors in the power law of wind profiles

Factors	Average time interval					
	1 hour	10 min.	1 min	15 s	5 s	3 s
α	1.000	1.060	1.180	1.260	1.310	1.330
β	0.150	0.130	0.113	0.106	0.102	0.100

4. Description of Computer Program TERMSIM

For computations the time domain program TERMSIM (TERMinal SIMulation) is used. For the combined equations of wave frequency and low frequency motion reference is made by Wihcers (1988). The program is well validated with model tests (Oortmerssen *et al.*, 1986). The carrier can be exposed to arbitrary weather conditons. The frequency domain computed linear first order RAO's (added mass, damping and wave forces) and the matrix of the quadratic second order wave drift force RAO's (incl. wave set-down in shallow water) are the input for convolution integrals and retardation function (Oortmerssen, 1976; Pinker, 1980). The hydrodynamic data, i. e. the matrices of the added mass and damping, the RAO's of the wave forces and the matrix of the quadratic transfer function of the wave drift forces, are computed by means of the 3-D potential theory program DIFFRAC.

Since for moored carriers the low frequency motions are resonance motions, the values of the low frequency hydrodynamic reactive forces / moment are important. In order to predict correctly these motions, an experimentally determined database is used which contains the low frequency hydrodynamic viscous (non-linear) coefficients for a large number of carriers, loading conditions and water depth / draft ratio (Wichers, 1988).

Further different wind spectrum formulations can be applied. For the wind and current loads the OCIMF data as given in References (OCIMF, 1985 and 1994) can be used.

Besides the non-linear load-elongation of the synthetic lines, the load-compression curve of the fenders is taken into account. Especially for the low frequency motions of the carrier the friction between the shiphull side and the fenders is important. For the friction a Colomb friction coefficient $k = 0.1$ is taken into account. The computations are carried out in the time domain.

For a carrier moored to a jetty the yaw and sway motions can be considered to be relatively small; this is in contradiction with carriers moored for instance by a hawser to a buoy (SPM) or in a spread mooring system. For a carrier moored to a jetty the equations of motion can be simplified as follows:

$$m\ddot{x}_1 + \sum_{k=1}^{6} a_{1k}\ddot{x}_k + \sum_{k=1}^{6} \int_{-\infty}^{t} R_{1x}(t-\tau)\dot{x}_k(\tau)\,d\tau_1 = F_1^{\text{wind}} + F_1^{\text{stat}} + F_1^{\text{dyn}} + F_1^{\text{wave}} + F_1^{\text{moor}}; \quad (5)$$

$$m\ddot{x}_2 + \sum_{k=1}^{6} a_{2k}\ddot{x}_k + \sum_{k=1}^{6} \int_{-\infty}^{t} R_{2k}(t-\tau)\dot{x}_k(\tau)\,d\tau$$

$$= F_2^{\text{wind}} + F_2^{\text{stat}} + F_2^{\text{dyn}} + F_2^{\text{wave}} + F_2^{\text{moor}} ; \tag{6}$$

$$m \ddot{x}_3 + \sum_{k=1}^{6} a_{3k} \ddot{x}_k + \sum_{k=1}^{6} \int_{-\infty}^{t} R_{3x}(t-\tau) \dot{x}_k(\tau)\, d\tau + c_{33} x_3 + c_{35} x_3$$

$$= F_3^{\text{wave}} + F_3^{\text{moor}} ; \tag{7}$$

$$I_{44} \ddot{x}_4 + \sum_{k=1}^{6} a_{4k} \ddot{x}_k + \sum_{k=1}^{6} \int_{-\infty}^{t} R_{4k}(t-\tau) \dot{x}_k(\tau)\, d\tau + c_{44} x_4 + b_{44} \dot{x}_4$$

$$= F_4^{\text{wave}} + F_4^{\text{moor}} ; \tag{8}$$

$$I_{55} \ddot{x}_5 + \sum_{k=1}^{6} a_{3k} \ddot{x}_k + \sum_{k=1}^{6} \int_{-\infty}^{t} R_{5k}(t-\tau) \dot{x}_k(\tau)\, d\tau + c_{55} x_5 + b_{55} x_5$$

$$= F_5^{\text{wave}} + F_5^{\text{moor}} ; \tag{9}$$

$$I_{66} \ddot{x}_6 + \sum_{k=1}^{6} a_{6k} \ddot{x}_k + \sum_{k=1}^{6} \int_{-\infty}^{t} R_{6k}(t-\tau) \dot{x}_k(\tau)\, d\tau$$

$$= F_6^{\text{wind}} + F_6^{\text{stat}} + F_6^{\text{dyn}} + F_6^{\text{wave}} + F_6^{\text{moor}} ; \tag{10}$$

in which, m, I — tanker mass and moment of inertia; a_{ik} — matrix of the frequency-independent added mass coefficients for $i = 1$ to 6 and $k = 1$ to 6; b_{44} — viscous roll damping coefficient; R_{ik} — matrix of the retardation functions; c_{ik} — matrix of the hydrostatic restoring force coefficients; F_i^{wind} — relative wind force in i direction; F_i^{stat} — relative current force in i direction; F_i^{dyn} — dynamic current force contributions in i direction; F_i^{wave} — first and second order wave force registrations in i direction; F_i^{moor} — mooring force due to fenders and mooring lines in i direction ($i = 1, 2, 6$).

Each computation starts with a transient time of half an hour followed by the period of 3 hours, for which the statistical results are derived. As an example time registrations of the forces in fender $3^{\#}$ as computed during the runs of weather conditions 5 and 9 are presented in Figs. 2 and 3. During each simulation the following signals are computed and analyzed:

- motions of manifold in surge direction X_{rel};
- motions of manifold in sway direction Y_{rel};
- motions of manifold in heave direction Z_{rel};
- roll motion of carrier;
- pitch motion of carrier;

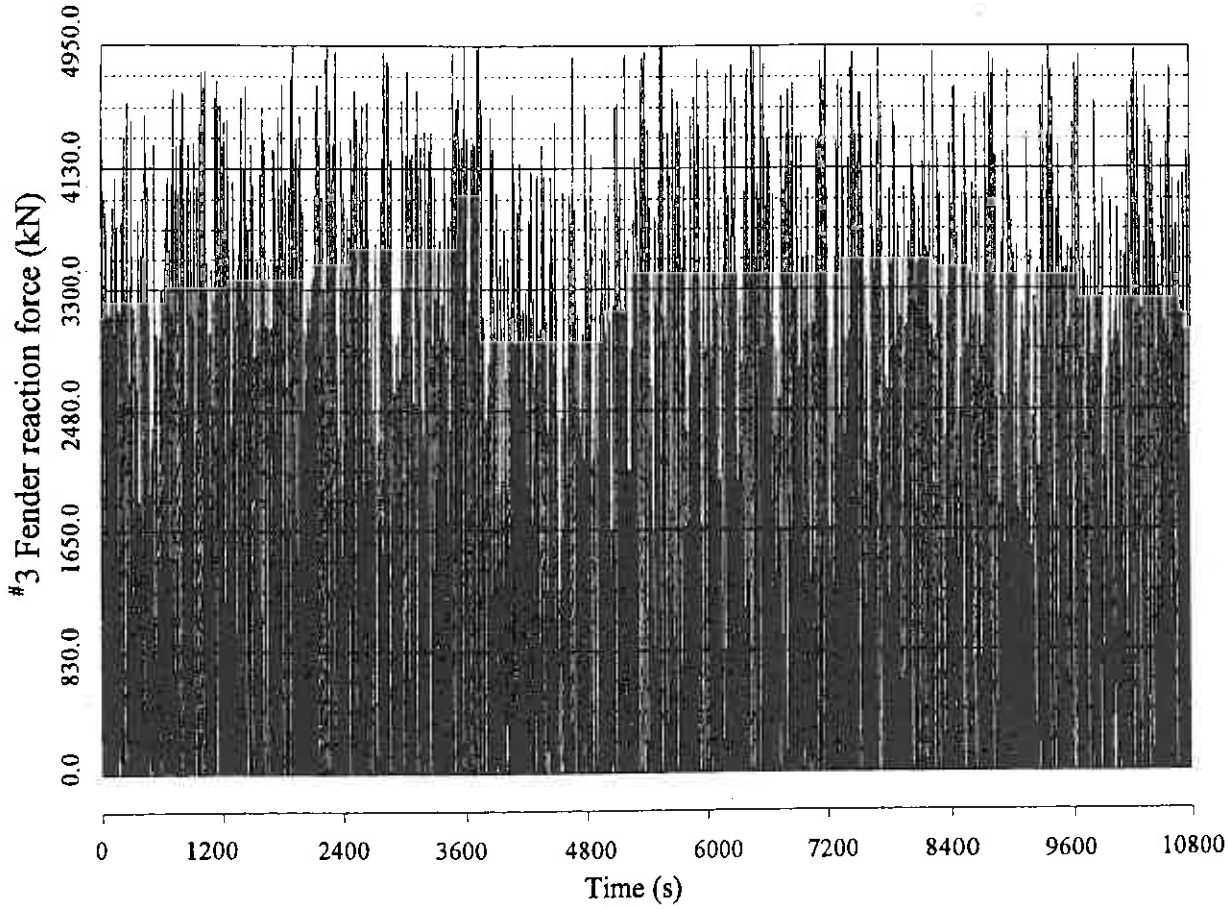

Fig. 2. Fender force in weather condition case 5.

- yaw motion of carrier;
- forces in lines $1^{\#}$ through $14^{\#}$;
- forces in fenders $1^{\#}$ through $4^{\#}$.

5. Discussion of Results

The results of computations in terms of mean, standard deviation and the maximum values are given in Tables 5 and 6. Some discussions are given through application of parameters of weather conditions.

5.1 Weather Conditions Case 1, Case 2 and Case 3

Under weather conditions case 1, case 2 and case 3 the mean wave period of the spectra is varied. Referring to the values as given in Tables 5 and 6, notice the results of the signals of the surge motions of the manifold, the forces in mooring lines and the forces on the fenders. The magnitude of the mean standard deviation (σ) and the maximum, except for the fender forces, clearly show that they increase with the increase of wave period. The reason for the increase of the surge motion and the line forces is the values of the matrix of the quadratic transfer function (QTF) of the wave drift forces / moment. As an example, the QTF of the mian diagonal of the

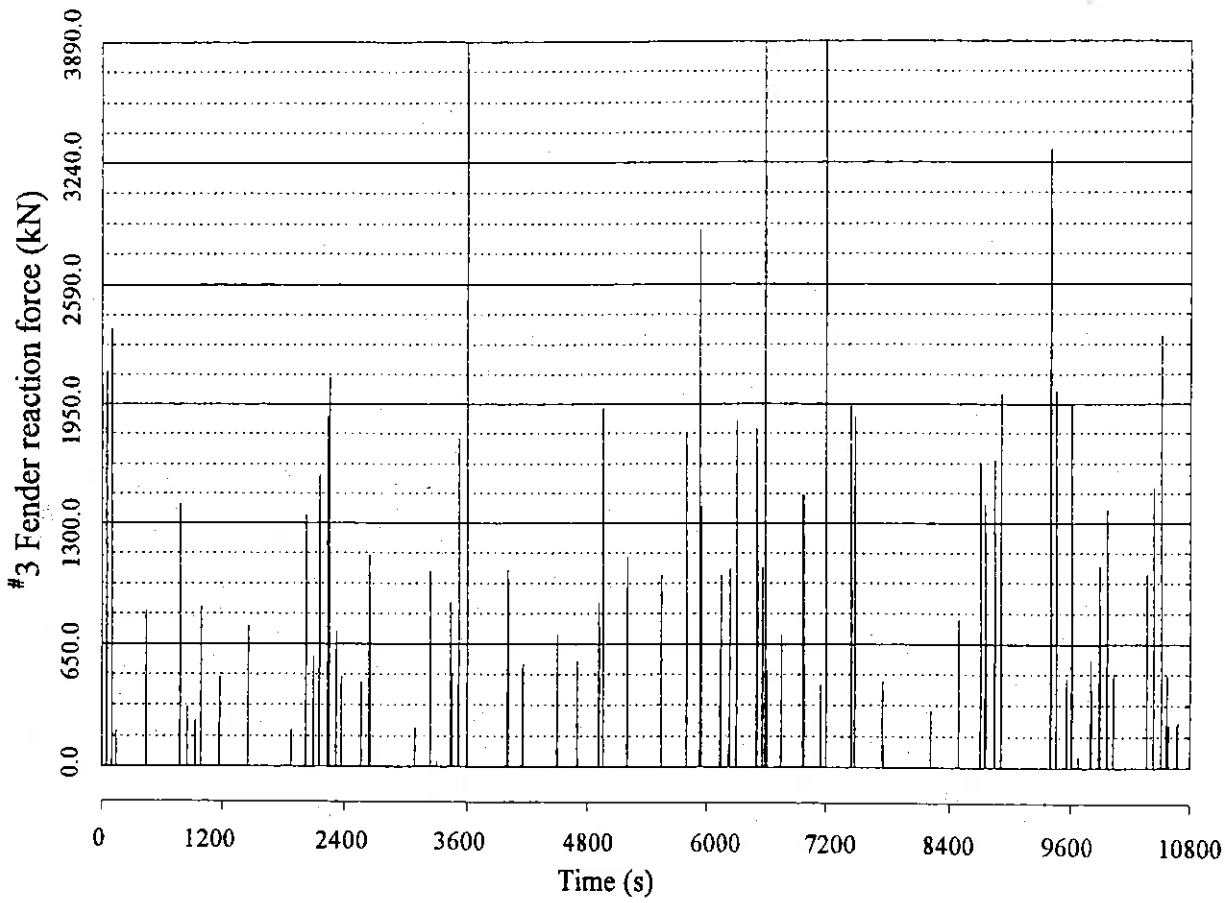

Fig. 3. Fender force in weather condition case 9.

wave drift force in x-direction under 135 ° wave directions is given in Fig. 4. From Fig. 4 it can be seen that the magnitude of the QTF increases from $\omega = 0.75$ rad / s ($T_p = 8.4$ s) to $\omega = 0.58$ rad / s ($T_p = 10.8$ s) with approximately a maximum value at $\omega = 0.48$ rad / s ($T_p = 13.2$ s). The mean wave drift force and the spectral density of the wave drift force are responsible for the mean and low frequency motions. They can be determined as follows:

$$\begin{cases} F_{1\text{mean}} = 2 \cdot \int_0^\infty S_\zeta(\omega)\, P(\omega, \omega)\, d\omega \\ S_F(\mu) = 8 \cdot \int_0^\infty S_\zeta(\omega)\, S_\zeta(\omega + \mu)\, T^2(\omega,\ \omega + \mu)\, d\omega \end{cases} \tag{11}$$

in which

$$T^2(\omega + \mu,\ \omega) = P^2(\omega + \mu,\ \omega) + Q^2(\omega + \mu,\ \omega);$$

μ — frequency of low frequency second order force;

$P^2(\omega + \mu, \omega)$, $Q^2(\omega + \mu, \omega)$ — in-phase and out-phase components of the quadratic transfer function;

$T(\omega + \mu, \omega)$ — amplitude of quadratic transfer function.

Table 5 Results of computations of mean value

Signals	Weather conditions									
	Run case 1	Run case 2	Run case 3	Run case 4	Run case 5	Run case 6	Run case 7	Run case 8	Run case 9	Run case 10
X_{rel} (m)	−0.53	−0.49	−0.37	−0.37	−0.41	−0.29	−0.42	−0.37	−0.38	−0.31
Y_{rel} (m)	−0.11	−0.004	0.04	−0.03	−0.07	−0.10	−0.39	−0.20	−0.46	−0.30
Z_{rel} (m)	0.006	0.01	0.01	0.01	0.01	0.00	−0.03	−0.02	−0.04	−0.03
Roll (°)	0.01	0.03	0.04	0.02	0.02	−0.00	−0.10	−0.07	−0.41	−0.09
Pitch (°)	0.00	0.00	0.00	0.00	0.00	0.00	0.00	0.00	−0.46	0.00
Yaw (°)	0.02	0.02	0.00	0.00	0.00	−0.01	−0.09	−0.05	0.00	−0.05
Line 1 / 2 (kN)	122	84	78	93	99	108	109	102	117	118
Line 3 / 4 (kN)	177	127	109	126	138	137	148	134	156	150
Line 5 (kN)	147	107	94	111	120	124	135	121	144	138
Line 6 / 7 (kN)	236	214	191	190	199	178	210	203	201	182
Line 8 / 9 (kN)	79	62	81	87	78	101	107	113	112	111
Line 10 (kN)	179	148	135	147	158	160	241	194	256	209
Line 11 / 12 (kN)	164	125	118	130	144	151	233	183	252	204
Line 13 / 14 (kN)	197	166	152	160	172	168	248	203	259	213
Fender 1 (kN)	1061	938	839	822	940	816	196	342	130	322
Fender 2 (kN)	893	868	1132	740	785	658	140	265	78	226
Fender 3 (kN)	1085	1107	1182	861	1053	812	343	135	177	99
Fender 4 (kN)	1280	1213	500	958	1198	954	424	165	283	140

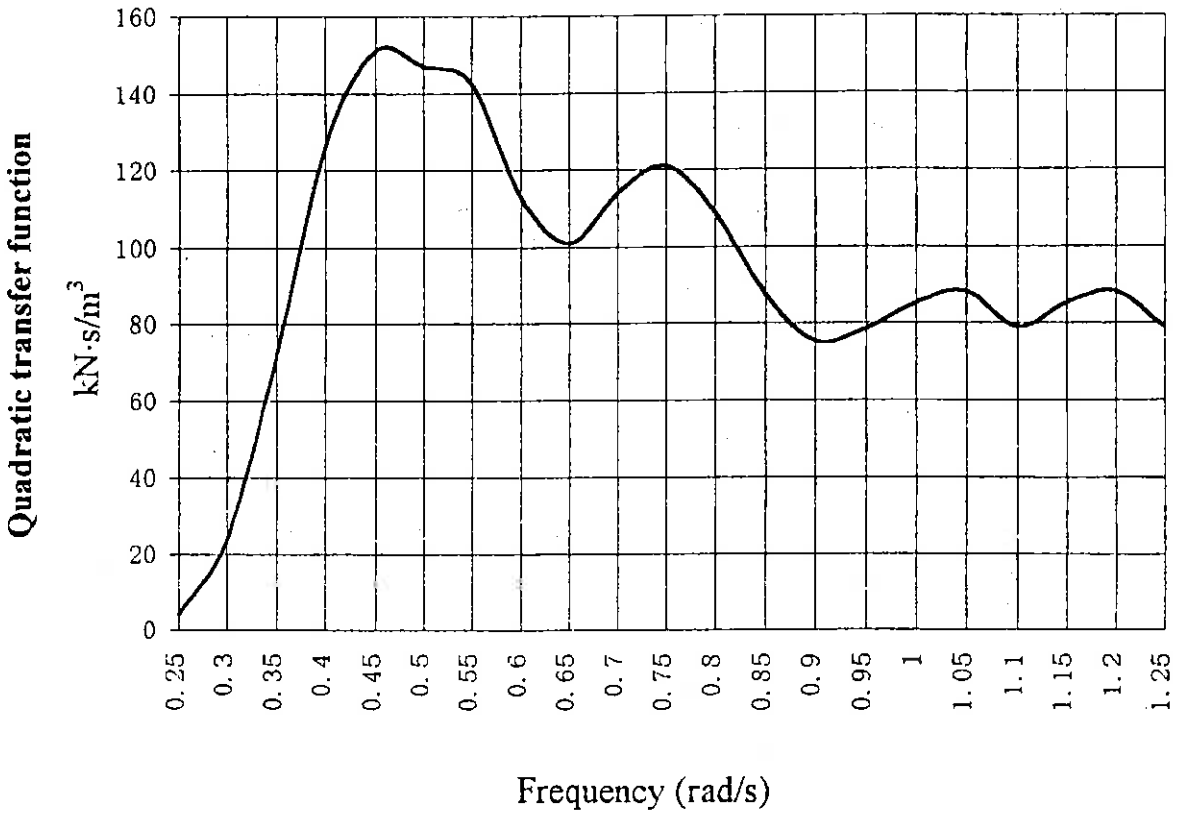

Fig. 4. Quadratic transfer function of wave drift force in x-direction (135° wave direction)

Considering these formulas it is clear that the excitation will increase if the peak period of the wave spectrum increase from T_p = 8.4 s to 13.2 s, resulting in higher values of motions and line forces. At the high load level the compression force will be constant over a relatively large range. For this reason it can be concluded that in most weather conditions the maximum fender force will mostly remain at the same level.

5.2 Weather Conditions Case 2, Case 4 and Case 6

For weather conditions case 2, case 4 and case 6 the parameters wind spectra and swell both are applied. The wind direction is 135 ° . Also notice the results as mentioned above.

A comparison of the results for weather conditions case 2 and case 4 (constant wind speed 25.2 m / s versus the mean hour of 20 m / s in combination with an API wind spectrum) shows that only the maximum values of the manifold motions and the line forces are 10 ~ 20% higher for a wind spectrum. For the fender force the same can be concluded as mentioned earlier. From a comparison of the results for weather conditions case 2 and case 5 it can be concluded that for the forces in the mooring lines both the standard deviation and the maximum values are significantly larger. In spite of the lowering of the sgnificant wave height, the effect of the resulting action of the remaining waves, swell and wind coming from the same direction seems to cause the increase in line forces. A comparison of the results for weather conditions case 5 and case 6 leads to the same conclusions as drawn for the results for weather conditions case 2 and case 4. For the fender force the same can be concluded as mentioned above.

5.3 Weather Conditions Case 7, Case 8, Case 9 and Case 10

For weather conditions case 7, case 8, case 9 and case 10 the parameters wind spectra and swell both are applied. The wind direction, however, is changed to 225 ° In this condition the wind has the effect of pushing the carrier away from the jetty.

From the results it can be concluded that the standard deviation and maximum values of both the motions of the manifold and the mooring line forces are significantly larger than those found under weather conditions case 2, case 4, case 5 and case 6. Owing to the changed wind direction, the carrier is less heavily pushed against the fenders as demonistrated in Figs. 2 and 3. The result is that the effect of the friction between the hull and the fender will be smaller, resulting in significantly larger low frequency motions. The effect of larger motions induces higher values of the forces in the mooring lines, especially in the spring lines compared with weather conditions case 2, case 4, case 5 and case 6.

The effect of the wind spectrum and the swell is not so significant with regard to the standard case as found in the case of wind direction 135 ° . This shows that it is important to consider wind direction in jetty design.

6. Conclusions

From the study of the sensitivity of the mooring system and carrier motions to the combinations of waves with and without swell, steady wind and wind spectra and with the wind directions of 135 ° and 225 ° the following conclusions can be drawn:

Table 6 Results of computations of standard deviation and maximum value

Signals	Weather conditions									
	Run case 1		Run case 2		Run case 3		Run case 4		Run case 5	
	σ	Max.	σ	Max.	σ	Max.	σ	Max.	σ	Max.
X_{rel} (m)	0.60	−3.65	0.26	−2.27	0.13	−1.04	0.28	−2.39	0.21	−1.57
Y_{rel} (m)	0.22	−1.23	0.17	−0.8	0.08	0.35	0.17	−0.90	0.18	−0.9
Z_{rel} (m)	0.16	0.69	0.11	0.51	0.26	0.24	0.10	0.47	0.10	0.42
Roll (°)	0.31	−1.36	0.27	−1.16	0.14	0.62	0.28	1.57	0.27	−1.2
Pitch (°)	0.25	1.06	0.14	0.6	0.07	−0.26	0.14	0.60	0.13	−0.58
Yaw (°)	0.35	−1.2	0.15	0.6	0.07	−0.26	0.15	0.58	0.25	−0.82
Line 1 / 2 (kN)	150	1785	63	511	24	180	65	610	92	847
Line 3 / 4 (kN)	192	1899	75	588	29	222	75	602	115	1066
Line 5 (kN)	158	1700	67	534	22	188	68	507	99	905
Line 6 / 7 (kN)	156	2385	53	789	23	312	57	871	43	528
Line 8 / 9 (kN)	92	1238	43	268	28	186	49	330	47	323
Line 10 (kN)	124	1029	55	465	32	239	56	481	86	588
Line 11 / 12 (kN)	152	1542	64	421	36	246	65	437	105	866
Line 13 / 14 (kN)	133	1142	56	580	31	263	58	612	85	552
Fender 1 (kN)	1590	5522	1228	4948	747	3781	1150	4945	1318	4948
Fender 2 (kN)	1423	5097	1150	4945	719	3508	1066	4933	1197	4947
Fender 3 (kN)	1511	4949	1269	4884	1137	4572	1124	4862	1435	4949
Fender 4 (kN)	1704	4949	1369	4902	1205	4672	1226	4879	1590	4949

Signals	Weather conditions									
	Run case 6		Run case 7		Run case 8		Run case 9		Run case 10	
	σ	Max.	σ	Max.	σ	Max.	σ	Max.	σ	Max.
X_{rel} (m)	0.23	−1.65	0.60	−3.1	0.69	−3.45	0.53	−2.50	0.37	−2.17
Y_{rel} (m)	0.19	−0.97	0.28	−1.29	0.23	−1.03	0.26	−1.38	0.25	−1.38
Z_{rel} (m)	0.10	0.40	0.09	0.34	0.08	−0.43	0.09	−0.40	0.09	−0.36
Roll (°)	0.28	−1.26	0.41	1.58	0.38	1.58	0.36	−1.41	0.33	−1.43
Pitch (°)	0.13	−0.58	0.14	0.6	0.14	0.60	0.14	−0.59	0.13	−0.58
Yaw (°)	0.24	−0.88	0.17	−0.73	0.15	−0.62	0.20	−0.73	0.21	−0.87
Line 1 / 2 (kN)	93	962	87	711	82	837	92	668	93	1032
Line 3 / 4 (kN)	112	1059	91	691	81	677	104	959	111	1129
Line 5 (kN)	98	964	86	699	76	732	94	784	98	1060
Line 6 / 7 (kN)	48	552	128	1132	156	1466	108	1016	73	762
Line 8 / 9 (kN)	50	394	99	802	113	1080	91	618	67	541
Line 10 (kN)	86	630	66	653	69	769	75	770	84	831
Line 11 / 12 (kN)	106	990	80	921	72	584	97	845	102	933
Line 13 / 14 (kN)	85	615	75	930	86	1126	79	912	86	865
Fender 1 (kN)	227	4946	668	4947	828	4936	520	4889	811	4769
Fender 2 (kN)	1052	4949	554	4948	716	4941	389	4662	649	4570
Fender 3 (kN)	1250	4949	233	3930	457	4409	159	3887	406	4126
Fender 4 (kN)	1417	4949	272	3988	525	4587	215	4110	517	4202

Table 6 Results of computations of standard deviation and maximum value

Signals	Weather conditions									
	Run case 1		Run case 2		Run case 3		Run case 4		Run case 5	
	σ	Max.	σ	Max.	σ	Max.	σ	Max.	σ	Max.
X_{rel} (m)	0.60	−3.65	0.26	−2.27	0.13	−1.04	0.28	−2.39	0.21	−1.57
Y_{rel} (m)	0.22	−1.23	0.17	−0.8	0.08	0.35	0.17	−0.90	0.18	−0.9
Z_{rel} (m)	0.16	0.69	0.11	0.51	0.26	0.24	0.10	0.47	0.10	0.42
Roll (°)	0.31	−1.36	0.27	−1.16	0.14	0.62	0.28	1.57	0.27	−1.2
Pitch (°)	0.25	1.06	0.14	0.6	0.07	−0.26	0.14	0.60	0.13	−0.58
Yaw (°)	0.35	−1.2	0.15	0.6	0.07	−0.26	0.15	0.58	0.25	−0.82
Line 1 / 2 (kN)	150	1785	63	511	24	180	65	610	92	847
Line 3 / 4 (kN)	192	1899	75	588	29	222	75	602	115	1066
Line 5 (kN)	158	1700	67	534	22	188	68	507	99	905
Line 6 / 7 (kN)	156	2385	53	789	23	312	57	871	43	528
Line 8 / 9 (kN)	92	1238	43	268	28	186	49	330	47	323
Line 10 (kN)	124	1029	55	465	32	239	56	481	86	588
Line 11 / 12 (kN)	152	1542	64	421	36	246	65	437	105	866
Line 13 / 14 (kN)	133	1142	56	580	31	263	58	612	85	552
Fender 1 (kN)	1590	5522	1228	4948	747	3781	1150	4945	1318	4948
Fender 2 (kN)	1423	5097	1150	4945	719	3508	1066	4933	1197	4947
Fender 3 (kN)	1511	4949	1269	4884	1137	4572	1124	4862	1435	4949
Fender 4 (kN)	1704	4949	1369	4902	1205	4672	1226	4879	1590	4949

Signals	Weather conditions									
	Run case 6		Run case 7		Run case 8		Run case 9		Run case 10	
	σ	Max.	σ	Max.	σ	Max.	σ	Max.	σ	Max.
X_{rel} (m)	0.23	−1.65	0.60	−3.1	0.69	−3.45	0.53	−2.50	0.37	−2.17
Y_{rel} (m)	0.19	−0.97	0.28	−1.29	0.23	−1.03	0.26	−1.38	0.25	−1.38
Z_{rel} (m)	0.10	0.40	0.09	0.34	0.08	−0.43	0.09	−0.40	0.09	−0.36
Roll (°)	0.28	−1.26	0.41	1.58	0.38	1.58	0.36	−1.41	0.33	−1.43
Pitch (°)	0.13	−0.58	0.14	0.6	0.14	0.60	0.14	−0.59	0.13	−0.58
Yaw (°)	0.24	−0.88	0.17	−0.73	0.15	−0.62	0.20	−0.73	0.21	−0.87
Line 1 / 2 (kN)	93	962	87	711	82	837	92	668	93	1032
Line 3 / 4 (kN)	112	1059	91	691	81	677	104	959	111	1129
Line 5 (kN)	98	964	86	699	76	732	94	784	98	1060
Line 6 / 7 (kN)	48	552	128	1132	156	1466	108	1016	73	762
Line 8 / 9 (kN)	50	394	99	802	113	1080	91	618	67	541
Line 10 (kN)	86	630	66	653	69	769	75	770	84	831
Line 11 / 12 (kN)	106	990	80	921	72	584	97	845	102	933
Line 13 / 14 (kN)	85	615	75	930	86	1126	79	912	86	865
Fender 1 (kN)	227	4946	668	4947	828	4936	520	4889	811	4769
Fender 2 (kN)	1052	4949	554	4948	716	4941	389	4662	649	4570
Fender 3 (kN)	1250	4949	233	3930	457	4409	159	3887	406	4126
Fender 4 (kN)	1417	4949	272	3988	525	4587	215	4110	517	4202

— In weather conditions case 1, case 2 and case 3, the values of motions of the manifold, and the forces in the mooring lines and fenders increase with the increase of the mean wave period of the spectra. This increases are caused by the quantitative form of the quadratic transfer function of the wave drift forces. Since the load-compression curve is constant over a large compression range the maximum values of the fender forces mostly remain at the same level.

— From a comparison of the results for weather conditions case 2 and case 4 it can be concluded that owing to the wind spectrum, the maximum values of manifold motions and line forces are 10～20% higher.

— From a comparison of the results for weather conditions case 2, case 5 and case 6 it can be concluded that, in spite of the lower wave height, the swell causes a significant increase of both the standard deviation and the maximum values of forces in the mooring lines.

— For weather conditions case 7, case 8, case 9 and case 10 it can be concluded that both the motions of the manifold and the forces in mooring lines are significantly larger than those for weather conditions case 2, case 4, case 5 and case 6.

— The wind directions is an important factor affecting the arrangement of the orientation of the jetty. The force in mooring lines and fenders could be affected by the changing of wind direction.

This study shows that computations are necessary in the finding and understanding of the sensitivity of resulting forces and motions to weather conditions for the design of a jetty.

References

OCIMF-Society of International Gas Tankers and Terminal Operators Ltd, 1985. *Prediction of wind loads on large liquefied gas carriers*, Witherby and Co. Ltd., London, England.

Wichers, J. E. W., 1988. *Simulation Model for Single Buoy Moored Tankers*, Ph. D. dissertation, Delft University of Technology, The Netherlands.

Oortmerssen, G. van, J. A. Pinkster and H. H. van den Boom, 1986. Computer Simulation of Moored Ship Behaviour, *Journal of Waterway, Port, Coastal and Ocean Engineering*, ASCE, **112**, 2.

Oortmerssen, G. van, 1976. *The Motions of a Moored Ship in Waves*, Ph. D. dissertation, Delf University of Technology.

Pinkster, J. A., 1980. *Low Frequency Second Order Wave Exciting Forces on Floating Structures*, Ph. D. dissertation, Delft University of Technology.

OCIMF, 1994. *Rediction of Wind and Current Loads on VLCC's*, Second Edition, Witherby and Co. Ltd., London, England.